Journal of Magnetic Resonance **137,** 29–32 (1999)
Article ID jmre.1998.1611, available online at http://www.idealibrary.com on IDEAL®

Fast NMR Flow Measurements in Plants Using FLASH Imaging

M. Rokitta,* U. Zimmermann,† and A. Haase*

**Physikalisches Institut, Lehrstuhl für Experimentelle Physik V (Biophysik); and †Biozentrum, Lehrstuhl für Biotechnologie, Universität Würzburg, Germany*

E-mail: rokitta@physik.uni-wuerzburg.de

Received March 18, 1998; revised September 15, 1998

A fast method for quantitative NMR imaging of flow velocities in intact plants is described. The purpose of this method is to observe dynamic changes of flow velocity in the xylem of plants after fast changes of environmental conditions. The spatial image resolution is 47 × 188 μm^2 in-plane. The method applies a fast gradient echo sequence (FLASH). Compared to other flow NMR imaging sequences, the imaging time was reduced by a factor of 6 with comparable signal-to-noise ratio. A complete flow measurement consists of a set of 8 different flow weighted images with a total acquisition time of 3.5 min. © 1999 Academic Press

Key Words: **NMR flow imaging; FLASH; microimaging; plants.**

1. INTRODUCTION

NMR is a useful tool for investigation of the mechanisms of long distance water transport in plants. Flow NMR imaging measures the flow velocity of water in a direct and noninvasive way. There are some special difficulties when dealing with plants: the flow velocities are in general low, down to 0.1 mm/s, the changes in flow velocity can occur within a few minutes, and the large amount of stationary water in the tissue compared with the flowing water in the vascular bundles causes partial volume effects and therefore dynamic range problems. Furthermore, large susceptibility differences due to air-filled spaces within the plant tissue result in short T_2^* times. Flow NMR imaging in plants has been successfully demonstrated by several authors (*1, 2*). However, rather long measurement times were needed as a spin-echo sequence was applied for the imaging part and each phase encoding step was flow encoded separately. This study demonstrates that a flow NMR sequence using FLASH imaging (*3*) can be applied to flow measurements in plants. A complete image with 32 phase encoding steps is acquired with only one flow encoding preparation step. In this way, the total measurement time can be reduced by a factor of 6 from 21 min to 3.5 min in a direct comparison with the method using spin-echo imaging (*4*) without a loss in signal-to-noise ratio.

2. MATERIALS AND METHODS

Ricinus communis plants, 35 to 40 days old, grown in quartz sand were used for the experiments (*5*). The size of the plants was about 24 cm; the imaging plane was chosen 8 cm above the sand surface. The flower pots had a diameter of 8 cm and a length of 18 cm. The experiments were performed on a 7 T Bruker BIOSPEC 70/20 horizontal bore magnet. The gradient system was capable of achieving maximal gradient strength of 196 mT/m with a rise time of 240 μs. The plants were installed in a homebuilt climate chamber (*4*) with full climate control and the possibility to measure transpiration and assimilation of the plant simultaneously with the NMR flow measurements. A Helmholtz-type radiofrequency coil with a diameter of 20 mm, tuned to the proton resonance frequency of 300 MHz, was used as transmitter and receiver coil.

The pulse sequence consists of two parts: flow encoding and imaging (see Fig. 1). As velocities down to 0.1 mm/s are to be measured, the flow encoding is done by a stimulated echo experiment with a gradient pulse separation time T of up to 200 ms (*6*). At the time the stimulated echo occurs, the fourth RF pulse (90°_y) flips the y-component of the magnetization back into the longitudinal direction (*7–9*). The phase shift φ between the flowing and the stationary spins which is responsible for the y-component of the magnetization depends on the flow velocity v, the strength G, and length τ of the flow encoding gradients and the time T between the two gradient pulses:

$$\varphi = \gamma G \tau T v. \qquad [1]$$

The remaining transverse magnetization is removed by a spoiler gradient. In this way, partial volume effects due to the large amount of stationary water can be avoided. In general, the vessels are smaller than the pixel dimensions. Assuming a laminar flow profile in these vessels, the signal depends on the average flow velocity $v_{avg} = v_{max}/2$ as (*8*)

$$S \propto \frac{\sin^2(\gamma G \tau T v_{avg})}{\gamma G \tau T v_{avg}} e^{-\gamma^2 G^2 D \tau^2 (T - \tau/3)}. \qquad [2]$$

The exponentially decaying part in Eq. [2] describes the attenuation of the NMR signal due to diffusion (*10, 11*). To reduce the total measurement time, a refocused FLASH imaging sequence (TE = 4.3 ms, TR = 11.5 ms, FOV = 6 × 6 mm^2,

1090-7807/99 $30.00

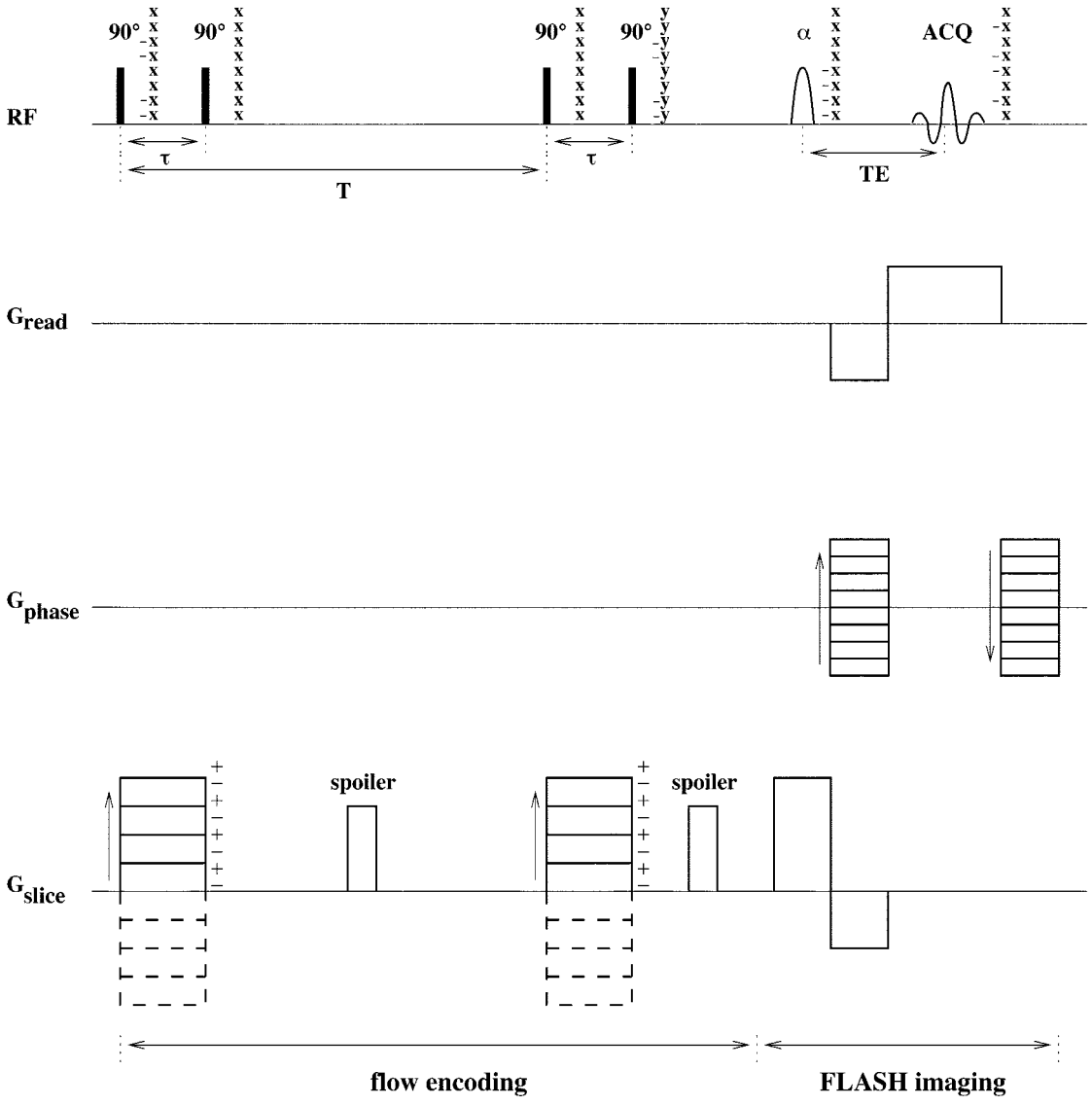

FIG. 1. Pulse sequence for the flow measurements: The phase cycle is indicated by a column of signed *x* or *y* symbols after each pulse together with a column of plus or minus signs for each of the flow encoding gradients. This means that every second step in the phase cycle, the flow encoding gradient is switched in the opposite direction together with a change in the pulse and receiver phases. All acquired signals add up—it is not a difference method. Typical values for the flow encoding are $\tau = 0.75$ ms, $T = 200$ ms, and $G_{max} = 172$ mT/m.

matrix = 128 × 32, slice = 4 mm, $T_{total} = 3.5$ min for 8 images, each with 16 averages) was used in the imaging part. In contrast to the spin-echo method where each phase encoding step has to be flow encoded separately, a whole image was obtained with one flow encoding step. The total measurement time is thus reduced, although FLASH imaging needs more averages than the spin-echo method to yield the same SNR. An effective phase cycle (see Fig. 1) is essential for good suppression of the stationary water signal.

For quantitative evaluation of flow velocities, a set of 8 different flow weighted images is acquired, each image averaged 16 times with 8-fold phase cycling (for details see Figs. 1 and 2). For evaluation of the datasets, a pixel-by-pixel fit of an appropriate function according to Eq. [2] is performed (*1*). The minimum detectable velocity v_{min} is limited by the fact that at least the first maximum of the $\sin^2 x/x$-function should be observed. The error of the fit increases if only a smaller part of the function is sampled. As the maximum values for G, τ, and T are limited by the gradient hardware, diffusion, and T_1-relaxation, the lower limit of the velocity is approximately 0.2 mm/s under the conditions described here.

3. RESULTS

Figure 2 shows a flow velocity map (colored) superimposed on the corresponding FLASH image (a) and spin-echo image (b). The FLASH and the spin-echo image, both acquired with-

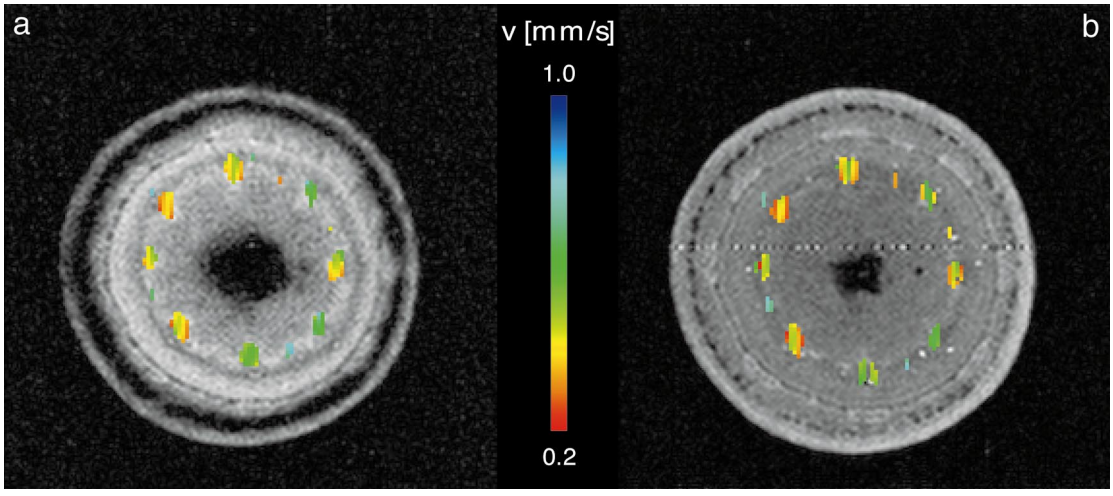

FIG. 2. Flow velocity maps (colored) superimposed on the corresponding (a) FLASH image (TE = 4.3 ms, TR = 11.5 ms, FOV = 6 × 6 mm^2, matrix = 128 × 32, slice = 4 mm, T_{total} = 3.5 min for 8 images with 16 averages) and (b) spin-echo image (TE = 11 ms, TR = 1 s, FOV = 6 × 6 mm^2, matrix = 128 × 32, slice = 4 mm, T_{total} = 21 min for 8 images with 4 averages).

out averaging on the same plant, show the same anatomical details. The cortex, phloem, xylem, and pith parenchyma can be clearly distinguished. The flow weighted images used for calculation of the velocity maps had a comparable signal-to-noise ratio in the case of FLASH and spin-echo imaging, respectively. The average flow velocities in eight different vascular bundles measured with both methods are compared in Table 1. They correspond in all bundles within the range of the standard deviation. The table also contains the SNR of the underlying images in these eight xylem regions and an average SNR value for the pith and the cortex parechyma. As the plants grow older, the eight discrete vascular bundles grow together to a ring. Therefore, it is understandable that flow also occurs between these bundles. It is interesting to note that the FLASH image and the spin-echo image, both acquired without averaging, show almost the same SNR in the xylem area, whereas the SNR of the FLASH image is worse in the cortex region. As can be seen on optical micrographs, the cells in the cortex region are smaller than in the pith region. Therefore, it can be expected that the T_2^* times are shorter than in the other tissues. An additional shortening of T_2^* might result from deposition of starch grains.

TABLE 1
Comparison of Average Flow Velocities and SNR in Eight Different Vascular Bundles of Fig. 2[a]

	FLASH		Spin-Echo	
No.	$\bar{v}\left(\frac{\text{mm}}{\text{s}}\right)$	SNR	$\bar{v}\left(\frac{\text{mm}}{\text{s}}\right)$	SNR
1	0.47 ± 0.07	12.8	0.46 ± 0.10	12.5
2	0.72 ± 0.09	12.4	0.60 ± 0.15	12.8
3	0.49 ± 0.09	12.4	0.44 ± 0.10	12.8
4	0.73 ± 0.09	12.4	0.68 ± 0.04	12.5
5	0.62 ± 0.04	12.5	0.60 ± 0.06	12.9
6	0.44 ± 0.08	12.4	0.42 ± 0.10	13.1
7	0.50 ± 0.07	12.8	0.51 ± 0.13	12.0
8	0.39 ± 0.06	12.4	0.37 ± 0.08	12.0
Pith	—	10.4	—	10.9
Cortex	—	2.5	—	10.6

[a] The numbers of the bundles start with the one on the top of each image and count clockwise. The SNR was determined in the underlying images without flow weighting by division of the signal in the region of interest by the standard deviation of the noise outside the object.

The flow measurements were performed over a total time period of three hours under different illumination conditions. Figure 3 displays the flow velocity in the xylem averaged over the whole stem cross-section. For averaging of flow velocities, only data points with nonzero values are taken into account. In the case of volume flow (velocity times signal amplitude of the flow weighted signal), data points with values of zero would also be considered. If the flow in larger parts of the stem cross-section stopped or fell to very low velocities, this would lead to significant changes in the volume flow rather than in the flow velocities. On the other hand, velocities are almost independent of most parameters that influence NMR images (e.g., relaxation times). In this measurement there was no appreciable difference in the time dependence of velocity and volume flow. The dotted vertical lines in the graph mark the former time resolution of 21 min. It can clearly be seen that most of the information about the time course of the changes would be lost with a time resolution of 21 min.

4. DISCUSSION AND CONCLUSION

The method presented here is the first one that offers sufficient temporal resolution to follow the time course of rapid

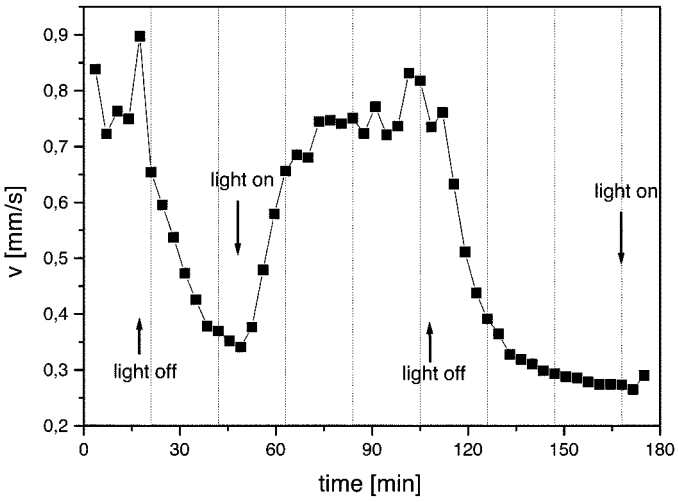

FIG. 3. Course of the flow velocity averaged over the whole xylem region. The total measurement time for one data point was 3.5 min. The dotted vertical lines mark the time intervals of 21 min, the time resolution of the previously used method (*4*) with spin-echo imaging.

changes of the flow velocities in the vascular bundles of *Ricinus communis* plants under preservation of high in-plane resolution of 47 × 188 μm. First experiments with tobacco plants (*Nicotiana tabacum*) also showed good results. The sequence might have its limitations in the investigation of plants with more air-filled spaces inside the stem. Because of the many alternating air–tissue interfaces, the T_2^* values are much less than 10 ms. Using a stronger gradient system, the echo time could significantly be reduced, and therefore the method might also work in these plants.

This method also allows the fast investigation of drought stress and rewatering. In first experiments, reactions of the plants on a similar time scale to that shown here were found. Such experiments might lead to a better understanding of the processes which allow plants to recover after heavy drought stress.

ACKNOWLEDGMENTS

Special thanks to A. Peuke for providing the plant material and help in botanical questions. The authors thank R. Deichmann, W. Landschütz, and K. Wolf for fruitful discussions. This work was supported by two grants from the Deutsche Forschungsgemeinschaft: Zi 99/9-2 and GRK 64/2.

REFERENCES

1. E. Kuchenbrod, M. Landeck, F. Thürmer, A. Haase, and U. Zimmermann, Measurement of water flow in the xylem vessels of intact maize plants using flow-sensitive NMR imaging, *Bot. Acta* **109(3),** 184–186 (1996).
2. P. T. Callaghan, W. Köckenberger, and J. M. Pope, Use of difference propagators for imaging of capillary flow in the presence of stationary fluid, *J. Magn. Reson. B* **104,** 183–188 (1994).
3. A. Haase, J. Frahm, D. Matthei, and K. D. Merbold, FLASH imaging: rapid NMR imaging using low flip angle pulses, *J. Magn. Reson.* **67,** 258–266 (1986).
4. W. Landschütz, M. Meininger, P. M. Jakob, F. Thürmer, U. Zimmermann, and A. Haase, In-vivo functional NMR imaging on plants at 7 T, *13th ESMRMB* **209,** 125 (1996).
5. A. D. Peuke, W. Hartung, and W. D. Jeschke, The uptake and flow of C, N and ions between roots and shoots in *Ricinus communis* L. II. grown with low or high nitrate supply, *J. Exp. Bot.* **45,** 733–740 (1994).
6. J. E. Tanner, Use of the stimulated echo in NMR diffusion studies, *J. Chem. Phys.* **52,** 2523–2526 (1970).
7. H. Lahrech, A. Briguet, D. Graveron-Demilly, E. Hiltbrand, and P. R. Moran, Modified stimulated echo sequence for elimination of signals from stationary spins in MRI, *Magn. Reson. Med.* **5,** 196–200 (1987).
8. D. Bourgeois and M. Decorps, Quantitative imaging of slow coherent motion by stimulated echoes with suppression of stationary water signal, *J. Magn. Reson.* **94,** 20–33 (1991).
9. A. Haase, M. Brandl, E. Kuchenbrod, and A. Link, Magnetization-prepared NMR microscopy, *J. Magn. Reson. A* **105,** 230–233 (1993).
10. H. Y. Carr and E. M. Purcell, Effects of diffusion on free precession in nuclear magnetic resonance experiments, *Phys. Rev.* **94,** 630–638 (1954).
11. E. O. Stejskal and J. E. Tanner, Spin diffusion measurements: Spin echoes in the presence of a time-dependent field gradient, *J. Chem. Phys.* **42,** 288–292 (1965).